Validation of Lower-Body Posture Prediction for the Virtual Human Model Santos™

Salam Rahmatalla, PhD; Yujiang Xiang; Rosalind Smith; John Meusch; Jinzheng Li; Tim Marler, PhD; Brian Smith
Center for Computer Aided-Design (CCAD)
The University of Iowa, Iowa City, Iowa 52242

ABSTRACT

A methodology is presented in this work to use inverse kinematics (IK) and optimization schemes to validate the lower extremity posture prediction capabilities of a predictive computer human model (Santos). In IK, the unknown joint angle profiles of a multi-skeletal human model were computed using matrix transformation, based on the Denavit and Hartenberg (DH) method and information obtained from the position of the end effectors and the location of various joint centers. Five subjects in seated and standing positions were instructed to reach targets using their lower extremities with their feet as end effectors. Qualitative and quantitative statistical analyses have shown considerable agreement between the predicted and the experimental results.

INTRODUCTION

Digital human modeling has attracted considerable attention in recent years, and this has heightened the need to model normal human movement due to its important role in many medical and industrial applications. The Virtual Soldier Research (VSR) Program at The University of Iowa has enriched the field of posture prediction with the development of Santos™, a new kind of virtual human [1-2]. Santos is a predictive computer human model that is not based on recorded data but can predict human motion and postures based on optimization schemes and laws of physics.

There are many attempts in the literature to model human movement [3-5]. For example, approaches that attempt to solve for human walking motions based on performance optimization [6-8] are shown to be suitable for reproduction of realistic human motions. In this case, objective functions are used to represent human performance measures, and optimization schemes are developed to solve for the feasible joint motion profiles that maximize the performance measures [9]. The works in this category are important because the human motions are not artificially constrained and are dynamically feasible.

One interesting characteristic of the optimization-based techniques is their tendency to introduce more than one feasible solution; this behavior is consistent with natural human behavior where people do tasks in various manners. If well formulated, the methodology may present optimal solutions that can be very useful for many applications such as training. However, the solution space of the optimization-based approaches can be narrowed down to obtain a one task-based solution. For example, in normal walking, the ranges of joint angle movement are well defined and therefore can be imposed as constraints to achieve natural motion.

There have been several attempts in the literature to validate the motion of digital human models [10]. However, most of these human models are based on experimental data and regression analyses that guide their motion; therefore, traditionally the validation process focuses on the statistical significance of these formulas to fit the experimental data.

There are many issues to be considered in validating the motion of human models. For example, Faraway [11] showed the effect of a precise and consistent definition of movement start and end points, which are required for comparison of motions across and within participants and targets. Others [11-13] have studied the effect of the variability in the motion time between different subjects and within the same subject when they conducted a similar task on the validation process. In this regard, they proposed a methodology to normalize the motion time and define t=0 to be the start of the motion and t=1 to be the end of the motion.

The challenge in the current work is to validate the motion of a predictive human model (Santos) whose motion is completely based on general equations of physics and some natural constraints. Besides the inertia forces, Santos's prediction is sensitive to the

effects of the external forces. Therefore, it is very important to choose a comparable environment for the model and the subjects during the validation process.

The objective of this article is to present the development of a framework to validate the capability of Santos to simulate normal human reaching activities using the lower extremities. Toward this end, a twelve-camera Vicon motion capture system was used to collect 3D motion data of five subjects reaching targets with their feet as end effectors.

MOTION CAPTURE PROCESS

There are many techniques and devices on the market for measuring 3D motion data. Examples include electromagnetic sensors, optical sensors, fiber-optic-based sensors, and inertia sensors. Some of these devices, such as the electromagnetic sensors, may suffer from interference problems with other equipment in the testing environment; others, such as fiber-optic-based and inertia sensors, are normally capable of producing only local information and therefore may need to be supplemented with global positioning devices such as gyroscopes. The optical sensors approach is both effective and efficient for collecting objective data for 3D motion analysis. Today, optical systems have many applications in biomechanical studies [14-15]. These systems have been shown to be accurate, repeatable, and consistent [16], and, as an additional benefit, there is no pain or risk involved in using such systems. In the motion capture process, a number of reflective markers are attached over bony landmarks on the participant's body, such as the elbow, the clavicle, or the vertebral spinous processes. As the participant walks or carries out a given physical task or function, the position history of each marker is captured using an array of infrared cameras.

There are many advantages to using optical motion capture systems to collect motion data. First, the markers are passive sensors, meaning that they are merely reflective surfaces and can be attached easily to any area on the body of the subject without requiring wires to connect them to a data collection system. Second, theoretically, only three markers are required to define the three-dimensional velocity and acceleration of each body segment. In this work, the time history of the location of the reflective markers was collected at a rate of 100 frames per second. Power spectrum analyses were conducted on the accelerometers' signals and a cut-off frequency of 8Hz was identified for subsequent data smoothing.

MARKER PLACEMENT PROTOCOL

Several marker protocols have been designed and used in various industries, including the entertainment, ergonomics, and medical sectors. The goal in most of these protocols is to define the location of the joint centers or to infer information about the relative motion between parts or all segments of the human body. The common scheme in all marker protocols is to track the motion of anatomical landmarks on the skin of the human body, from which useful information can be obtained about the skeleton motion underneath. Normally, the aim is to characterize the joint center location between adjacent segments or to identify the center of mass of a certain segment. While a marker protocol can be general and can be used for many applications, there are some situations where the protocol may have limitations or may fail to fulfill the test design requirements. To study the motion of the spine in a seated position in a car, for example, the markers on the back of the subject can be occluded from the camera scene; as a result, a special marker placement protocol should be designed and used for seated position scenarios [17].

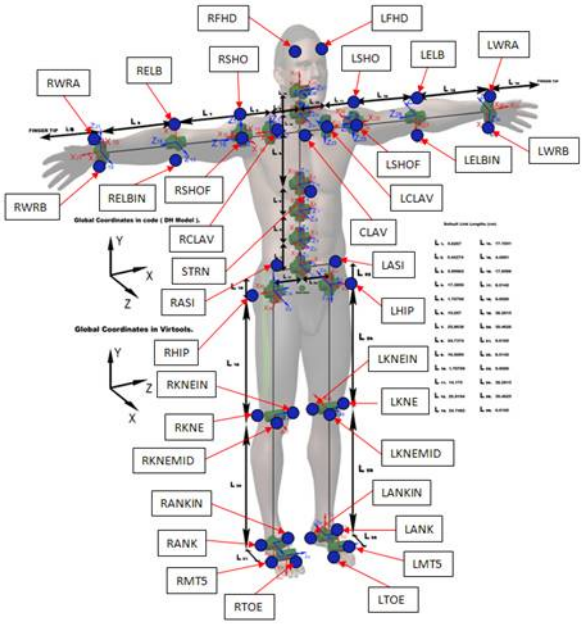

Figure 1: Frontal view of Santos marker placement protocol: blue circles represent reflective markers, and the text in the rectangular boxes presents acronyms of these markers; green cylinders represent joint center locations and degrees of freedom at each joint center. Fig. 3 shows a physical representation of the markers.

In this work, a marker placement protocol is developed by Center for Computer-Aided Design (CCAD) researchers. The proposed protocol is depicted in Fig. 1, where markers are placed on the subjects to highlight bony landmarks and identify segments between joints in line with previously identified guidelines and suggestions [18]. The skeleton of Santos includes the major joints present in the human body and is limited to four joints in the lumbar spine and two joints in the cervical spine.

In the protocol, markers were placed around joint centers to determine the instantaneous center of motion of each joint. For example, three markers were placed around the knee. One marker was placed directly on the medial epicondyle, another on the lateral epicondyle, and the third on the central anterior patellar surface. Each of these marker positions was identified as an

anatomical landmark by Cappozzo et al. [19] with the terminology coming from the well-defined, classic standards used by Gray and Lewis [20]. A similar technique was used for the remaining joints of the subject.

REACHING DETERMINANTS

After developing a protocol for collecting and processing the data, the next important phase in the validation process is to determine the minimum number of parameters that define a given posture at its end position; these parameters are identified to be the determinants of the posture. If Santos has the ability to predict each of these determinants within a statistically acceptable range, then he can execute the task in a natural way that is characteristic of human posture.

In this work, five degrees of freedom were chosen to represent the lower extremity reaching determinants. These include hip flexion/extension, hip abduction, hip rotation, knee flexion/extension, and ankle plantar/dorsiflexion. Figure 2 provides a graphical representation of some of the lower extremity reaching determinants. While pelvic motion is important and may affect the results, it will not be considered in this work and will be included in future work that deals with whole-body posture prediction.

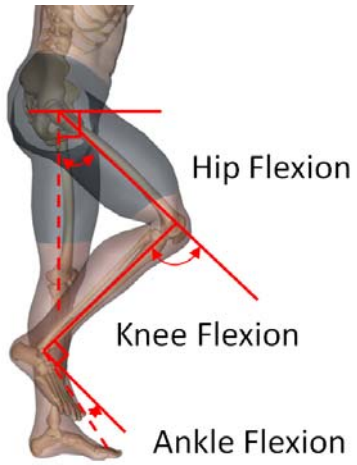

Figure 2: Pictorial depictions of some of the lower extremity determinants.

SUBJECT POPULATION

The subject population was comprised of five healthy subjects, three males and two females. The subjects had no history of musculoskeletal problems and were reasonably fit. Their participation was voluntary, and each subject signed a consent form before beginning the experiment. The mean height of the subject population was 5'9" with a mean weight of 145 lbs. The average age of the participants was 20 years old.

DATA COLLECTION

When a subject came in to the motion capture lab, he/she put on the motion capture suit (Velcro pants as shown in Fig. 3), and markers were placed on his/her body according to the previously defined marker placement protocol (Fig. 1). Bony landmarks were carefully located and corresponding markers were placed accordingly. While our methods for joint center calculations are defined based on anatomical detail, it is important that marker positions reflect these bony landmarks [19, 21].

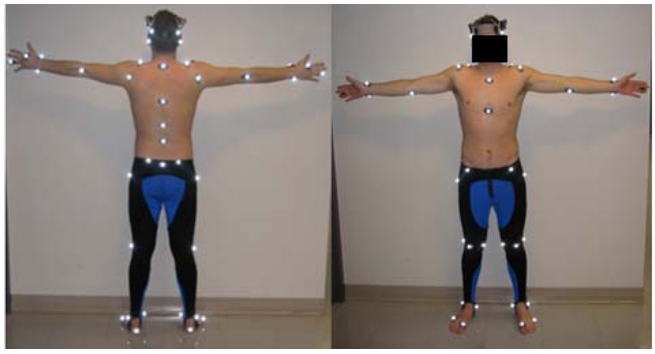

Figure 3: Subject standing in a t-pose.

In the experiments, the subjects were instructed to practice reaching severaltargets while they were in sitting and standing positions until they were comfortable with the camera setup. Each subject was instructed to reach targets using their feet as end effectors and as follows.

SITTING EXPERIMENTS

In this test, two target blocks were placed anterior to the frontal plane of the subject, one target for each foot. Each subject was seated on a stool 62 cm in height and directed to begin in a seated t-pose (Fig. 3), place their feet at a comfortable starting position, and then proceed to place their heels on the two target blocks. The subject's left foot was placed such that it rested on the block as it would on the floor of an automobile, and the right foot was placed to simulate placing it on the acceleration pedal. The right target block was marked with tape closest to the subject where they would rest their right heel. Both target blocks were adjusted so that each subject could rest their left foot and right heel comfortably taking into account individual subject anthropometries. Each target block was placed laterally, approximately 10 cm from the midline of the subject with a height of about 30 cm. Depending on the subject's anthropometry, the left target was placed 50-75 cm in front of the subjects and the right target was placed 65-85 cm anterior to the body as well.

STANDING EXPERIMENTS

In this portion of the study, two target blocks were placed in front of the subjects. The subjects were instructed to reach these targets with the ball of their right foot. To ensure marker visibility, each subject was instructed to start in the standing t-pose reference position for every trial. Next, the subjects grasped a post to assist with balance and reached each of the two targets left to right, pausing for approximately 3 seconds at each target. Between the targets, each subject was instructed to return to a neutral relaxed position before attempting to reach the subsequent target. Subjects were directed to proceed with a natural pace and given adequate practice to ensure each target was reached. Targets were arranged in a base position and adjusted slightly to accommodate individual anthropometries. The first target was placed approximately 47 cm anterior to the frontal plane, 32 cm to the left of the midline, and 52 cm above the floor plane. The second target was placed 47 cm forward and 23 cm to the right with a height of 23 cm.

END-EFFECTORS

In this study, each foot is considered as an end effector. Four markers were attached to the end effector to characterize its location and orientation. One marker was attached to the heel, the second was attached to the toe, and the last two markers were attached around the heel to specify the position of the heel's joint center. The positions of these markers, at the end posture, were used by the simulation software as the target points.

ANALYSIS

INVERSE KINEMATICS

In inverse kinematics, unknown joint angle profiles of a multi-skeletal model are computed using matrix transformation, based on information about the position of the end effectors and the location of various joint centers. In the case of the human body, the complexity of the structure and the large number of degrees of freedom involved causes tremendous difficulties in solving for joint angle profiles using inverse kinematics with traditional matrix transformation methods. This work presents optimization techniques to accommodate this problem.

In addition to the large number of degrees of freedom, there is another issue that needs to be addressed when using the inverse kinematic method: the geometrical relationship between adjacent coordinates in the skeleton. The skeleton of the computer human model (Santos) is developed and built based on the DH method (described in the following section); therefore, in order to create a comparable solution space for the joint angles between the simulation and the experiments, the same skeleton used for simulation will be used in the inverse kinematics formulation to solve for the experimental joint profiles.

Finally, the inverse kinematics method is well defined in robotics applications, and there is a clear definition of the joint centers and the assumption of constant link lengths. This situation becomes more delicate when dealing with the human skeleton, where there are many uncertainties about the location of the joint centers and the magnitude of the link lengths. Due to the complexity of the human skeleton, the joint center locations are not well defined and may change position during the motion. To avoid this problem in the current work, markers are placed around each joint center to trace an approximate instantaneous location of each joint center (Fig. 4) throughout the motion. Accordingly, the link lengths, which represent the Euclidean distance between the adjacent joint centers, are updated during the motion.

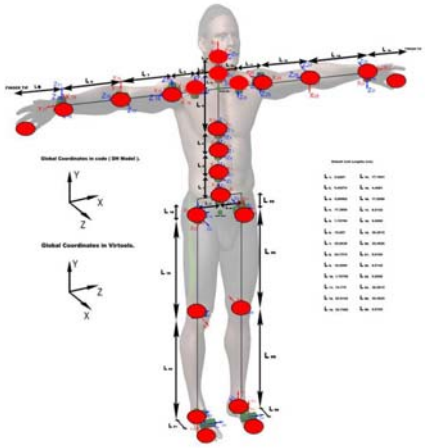

Figure 4: Skeletal model of Santos in the inverse kinematics process; the red elliptical shapes represent the location of the instantaneous joint centers and the end effectors during the motion.

Skeletal Model

The skeleton of the Santos human model is defined in the joint space with 55 degrees of freedom: 6 for global translation and rotation and 49 representing the kinematics of the body, as shown in Fig. 5.

The model consists of six physical branches and one virtual branch. The physical branches include the right leg, the left leg, the spine, the right arm, the left arm, and the head. In these branches, the right leg, the left leg, and the spine start from the pelvis, while the right arm, left arm, and head start from the ending joint of the spine (z_{30}, z_{31}, z_{32}). The virtual branch contains six global DOFs, including three global translations (z_1, z_2, z_3) and three global rotations (z_4, z_5, z_6) located at the pelvis, and move the model from the origin (o-xyz) to the current pelvic position (z_4, z_5, z_6).

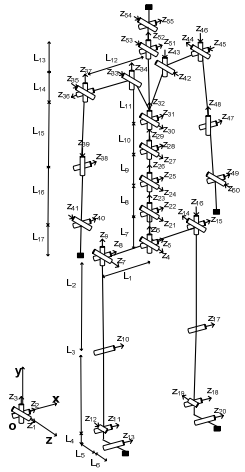

Figure 5: Santos skeletal model used in the predictive dynamics model; z stands for degrees of freedom and L represents link length.

Denavit-Hartenberg Method

The kinematics of the spatial human skeletal model in the current work is based on the DH method [22]. In the DH method, 4×4 homogeneous transformation matrices relate two adjacent coordinate systems. The DH transformation matrix includes rotation and translation and is a function of four parameters: θ_i, d_i, α_i, and a_i, as shown in Equation (1).

$$ {}^{i-1}\mathbf{T}_i = \begin{bmatrix} \cos\theta_i & -\cos\alpha_i \sin\theta_i & \sin\alpha_i \sin\theta_i & a_i \cos\theta_i \\ \sin\theta_i & \cos\alpha_i \cos\theta_i & -\sin\alpha_i \cos\theta_i & a_i \sin\theta_i \\ 0 & \sin\alpha_i & \cos\alpha_i & d_i \\ 0 & 0 & 0 & 1 \end{bmatrix} \quad (1) $$

In order to obtain a systematic representation of a serial kinematics chain, $\mathbf{q} \in R^n$ is defined as the vector of n-generalized coordinates, the joint angles. The position vector of a point of interest in the Cartesian space can be written in terms of the joint variables as $\mathbf{X} = \mathbf{X}(\mathbf{q})$. In this form, the augmented 4×1 vectors ${}^0\mathbf{r}_n$ and $\mathbf{r}_n$ are defined using the global Cartesian vector $\mathbf{X}(\mathbf{q})$ and the local Cartesian vector $\mathbf{X}_n$ as:

$$ {}^0\mathbf{r}_n = \begin{bmatrix} \mathbf{X}(\mathbf{q}) \\ 1 \end{bmatrix}; \qquad \mathbf{r}_n = \begin{bmatrix} \mathbf{X}_n \\ 1 \end{bmatrix} \quad (2) $$

where $\mathbf{X}_n$ is the position of a point with respect to the n^{th} coordinate system. Using these vectors, ${}^0\mathbf{r}_n$ can be related to $\mathbf{r}_n$ as follows:

$$ {}^0\mathbf{r}_n = {}^0\mathbf{T}_j(\mathbf{q})\ \mathbf{r}_n \quad (3) $$

$$ \begin{bmatrix} X_j(\mathbf{q}) \\ 1 \end{bmatrix} = {}^0\mathbf{T}_j(\mathbf{q}) \begin{bmatrix} \mathbf{r}_j \\ 1 \end{bmatrix} $$

where

$$ {}^0\mathbf{T}_n(\mathbf{q}) = \prod_{i=1}^{n} {}^{i-1}\mathbf{T}_i = {}^0\mathbf{T}_1(q_1)\,{}^1\mathbf{T}_2(q_2)\cdots{}^{n-1}\mathbf{T}_n(q_n) \quad (4) $$

PROBLEM DEFINITION

In this work, the joint angle profiles are computed as follows.

From the experimental data and at a given time, the locations of the reflective markers on the human subject are used to trace the position of the end effectors and different joint centers. Various link lengths are computed as the Euclidean distance between the adjacent joint centers between the segments. Based on this information, inverse kinematics is used to solve for a trail solution for the various joint angle profiles using the DH method. This is followed by an optimization problem, which is formulated as follows:

Minimize the error between the predicted and the experimental joint center and end effector positions, subjected to the natural limits on the various joint angles. A large-scale sequential quadratic programming (SQP) approach in SNOPT [23] was used to solve the optimization problem.

Design Variables

The design variables in this work are the joint profiles $q_i(t)$ for gait motion.

Objective Function

The norm of the error between the experimental and the calculated joint center locations is used as the objective and is as follows:

$$ \textit{Minimize} \qquad f(\mathbf{q}) = \left\| X_j(q) - \overset{*}{X}_j \right\| \quad j = 1, 2, ...n \quad (5) $$

where *n* is the number of degrees of freedom, $\overset{*}{X}_j$ is the experimental location of the *j* joint center, and $X_j(q)$ is the corresponding predicted joint center computed via inverse kinematics.

Constraints

The joint angle limits accounting for the physical range of motion, obtained from experiments, are considered as constraints for the current formulation:

$$ \mathbf{q}^L \le q_i \le \mathbf{q}^U \quad i = 1, 2, ..., 55 \quad (6) $$

where $\mathbf{q}^L$ is the lower limit of the joint angles and $\mathbf{q}^U$ is the upper limit of the joint angles.

Due to the significance of satisfying the location of the end effectors in a stricter manner, the norm of the latter was imposed as a constraint in the optimization problem:

$$\left\| X_k(q) - \overset{*}{X}_k \right\| \le \varepsilon \quad k = 1, 2, ...ne \tag{7}$$

where *ne* is the number of end effectors, $\overset{*}{X}_k$ is the experimental location of the *k* end effectors, $X_k(q)$ is the corresponding predicted end effectors computed via inverse kinematics, and ε is a small number.

SANTOS SIMULATION FORMULATION

For the simulation part of this work, the posture prediction problem was solved by finding q values, at the end posture, to minimize the displacement of the joints from a neutral standing posture subject to the end effector and joint limit constraints. ε is a small positive number approximating zero and $\mathbf{q}$ represent Santos degrees of freedom shown in Fig. 5.

The following problem is solved utilizing an optimization software (SNOPT) [23] using a sequential quadratic programming algorithm.

Find (design variables): $\mathbf{q} \in R^{DOF}$

to minimize (objective function): $f_{\text{JointDisplacement}}(\mathbf{q})$

subject to (constraints):

$$\text{distance} = \left\| \mathbf{x(q)}^{\textbf{end-effector}} - \mathbf{x}^{target-point} \right\| \le \varepsilon \tag{8}$$

$$q_i^L \le q_i \le q_i^U \;;\; i = 1, 2, ..., DOF$$

The joint displacement performance measure (objective function) is given below. Joint displacement is a weighted sum of the square of the displacement of each joint from the neutral position.

$$f_{\text{JointDisplacement}}(\mathbf{q}) = \sum_{i=1}^{n} w_i (q_i - q_i^N)^2 \tag{9}$$

RESULTS

Figures 6-8 demonstrate the resulting postures for both simulation (right side of the figures) and experiments (left side of the figures) during the reaching tasks (described in the Data Collection Section).

While the inverse kinematics scheme solves for the joint angle histories, our interest in this work is to investigate the end posture (a single frame), where the subjects reached their targets and held that position for three seconds.

Figure 6 depicts the resulting postures for the sitting scenario, where the subjects sat and reached two targets using their feet. Figures 7-8 show the resulting postures where the subjects stood and reached their targets using their feet. Figures 9-11 show radial graphs of the reaching determinants for the tasks depicted in Figs. 6-8. In each figure, each radial line represents a reaching determinant. So, there are ten radial lines representing 10 determinants (five for each leg).

The mean and the 95th percentile measures for each determinant were calculated and projected on the figures. The resulting points were connected together to form the shapes shown in the figures. Santos reaching determinants were also projected on the figures and are shown in red.

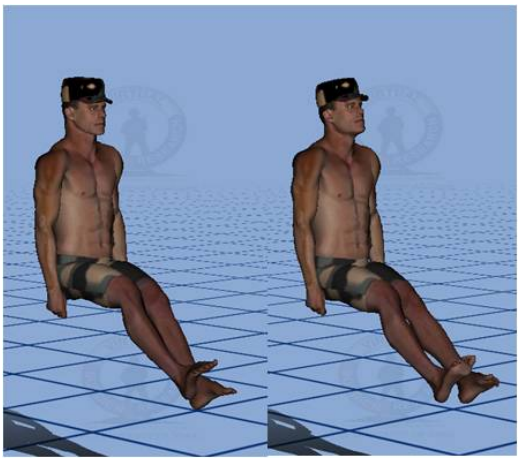

Figure 6: Reaching with both legs; right foot reaching the gas accelerator while the left foot rests on the floor. Right picture show predicted posture; left picture shows experiments.

Figure 7: Reaching with both legs; right foot reaching an academic target on the right side while left foot rests on the floor. Right picture shows predicted posture; left picture shows experiments.

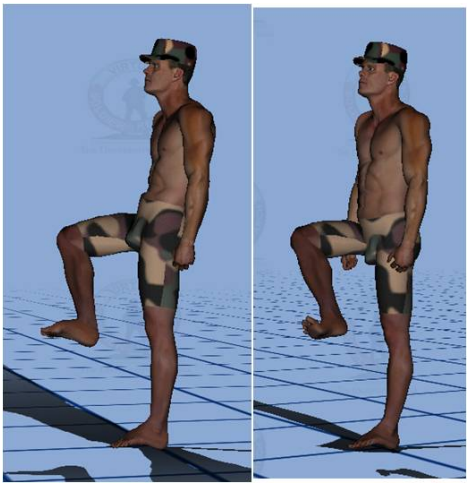

Figure 8: Reaching with both legs; right foot reaching an academic target on the left side while left foot rests on the floor. Right picture shows predicted posture; left picture shows experiments.

VALIDATION

QUALITATIVE COMPARISON

From Figs. 6, 7, and 8, we can qualitatively inspect the results for the final posture simulated by the subject during the motion capture experiments. For all tasks, the postures were visibly similar between simulated and experimental human data, although some minor toe differences can be seen between experimental and simulated postures. The toes consistently show a nuance in posture, being slightly rotated outward relative to the motion capture data, but the model maintains the same overall posture of the leg as in the experimental results. With a closer look (Fig. 8), we can recognize some differences in the pelvic area of the experimental posture. The pelvic motion will have significant impact on the resulting hip motion as shown in Figs. 10-11.

QUANTITATIVE COMPARISON

The comparison between the experimental results obtained from motion capture and the predicted results made by the virtual human Santos are presented in Figs. -11. If the simulation lies within the region of the upper and lower bounds of the interval of confidence, then a strong agreement is shown between the simulation and normal lower-body reaching. In other words, if the predicted values lie within the region, we can be 95% confident that Santos's digital model is capable of reliably representing normal lower-body reaching.

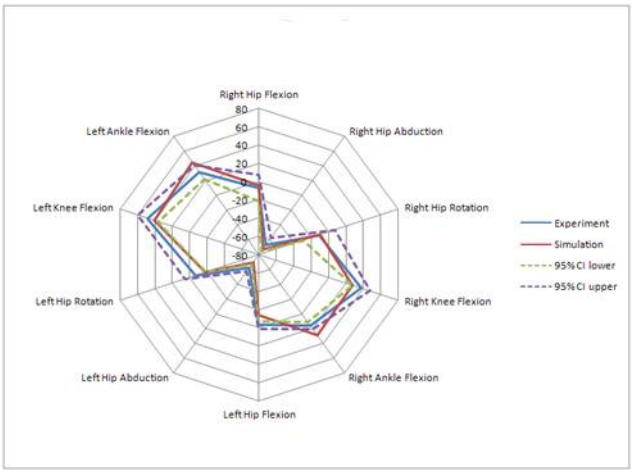

Figure 9: Lower extremity reaching determinants with the 95% interval of confidence, mean, and predicted posture for the scenario in Fig. 6. Ten radial lines represent ten determinants, five for each leg; each radial line represents a reaching determinant.

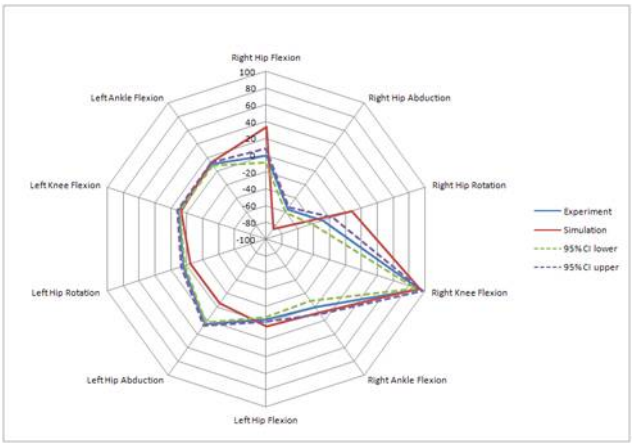

Figure10: Lower extremity reaching determinants with the 95% interval of confidence, mean, and predicted posture for the scenario in Fig. 7. Ten radial lines represent ten determinants, five for each leg; each radial line represents a reaching determinant.

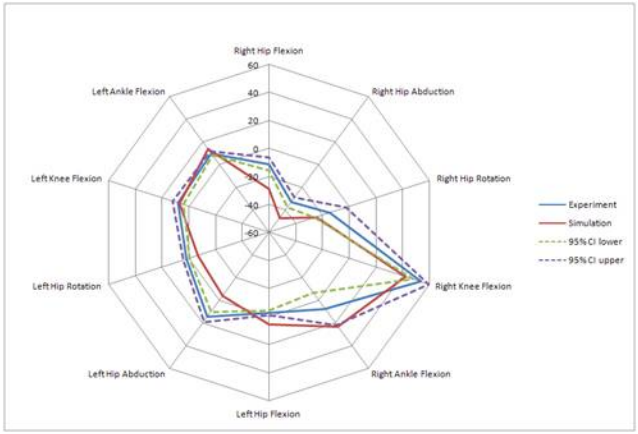

Figure11: Lower extremity reaching determinants with the 95% interval of confidence, mean, and predicted posture for the scenario in Fig. 8. Ten radial lines represent ten determinants, five for each leg; each radial line represents a reaching determinant.

With the first experiment, where the subjects were in sitting positions, Fig. 9 has shown that Santos's ankle plantar/dorsiflexion, for both right and left legs, is outside the interval of confidence of the subjects' population. This could be related to the small range of motion that the ankle encountered, therefore magnifying the error. Still, the curve shows a correlation to normal movement; better comparison may be obtained by increasing the subject populations and better matching the location of the center of the ankles between the experiment and the simulation.

With the standing experiments and the effect of pelvic movement, there were significant discrepancies in the hip motion, including hip flexion, abduction, and rotation. Therefore, it is important to consider the effect of the pelvic motion on the reaching determinants.

CONCLUSIONS AND DISCUSSIONS

This study provided the initial validation of the predicted reaching of the lower extremities by the virtual human model Santos. More importantly, it provided a logical and systematic approach to virtual human validation. The proposed method of validation is essential to the use and dependability of the model, so while it may be improved and expanded upon in the future, it has provided the foundation for predictive posture capabilities validation. Now that a systematic process has been defined and completed, it will be used to validate other dynamic human posture and motions predicted by Santos [26, 27].

ACKNOWLEDGMENTS

This research is funded partly by Virtual Soldier Research (VSR) partners. They include US Army TACOM, Caterpillar Inc., Natick Soldier Research Center, Honda R&D Americas Inc., and USCAR. We would like to thank all other research members within VSR for their contributions.

REFERENCES

1. Yang, J., Marler, T., Beck, S., Abdel-Malek, K., and Kim, J. (2006). Real-time optimal reach-posture prediction in a new interactive virtual environment. *Journal of Computer Science and Technology* 21(2), 189 – 198.Abdel-Malek, K., Yang, J., Kim, J., Marler, T., Beck, S., Swan, C., Frey-Law, L., Mathai, A., Murphy, C., Rahmatalla, S., and Arora, J. (2007). Development of the Virtual-Human Santos TM. Lecture Notes in Computer Science 4561, 490-499.
2. McGuan, S. (2001). Human Modeling – From Bubblemen to Skeletons, 2001 SAE Digital Human Modeling for Design and Engineering Conference, June 26-28, 2001, Arlington, Virginia.
3. Yamaguchi, J., Soga, E., Inoue, S., and Takanishi, A. (1999). Development of a bipedal humanoid robot control method of whole body cooperative dynamic biped walking. *IEEE International Conference on Robotics and Automation*, 1, 368-374.
4. Kajita, S., Kanehiro, F., Kaneko, K., Fujiwara, K., Harada, K., Yokoi, K., and Hirukawa, H. (2003). Biped walking pattern generation by using preview control of zero-moment point. *Proceedings of the IEEE International Conference on Robotics and Automation*, Taipei, Taiwan, 1620-1626.
5. Huang, Q., Yokoi, K., Kajita, S., Kaneko, K., Arai, H., Koyachi, N., and Tanie, K. (2001). Planning walking patterns for a biped robot. *IEEE Transactions on Robotics and Automation*, 17, 280-289.
6. Mu, X.P. and Wu, Q. (2003). Synthesis of a complete sagittal gait cycle for a five-link biped robot. Robotica, 21, 581-587.
7. Kim, H.J., Horn, E., Arora, J.S., and Abdel-Malek, K. (2005). An optimization-based methodology to predict digital human gait motion. 2005 Digital Human Modeling for Design and Engineering Conference, June 14 - 16, 2005, Iowa City.
8. Park, W., Chaffin, D.B., and Martin, B.J. (2004). Toward memory-based human motion simulation: Development and validation of a motion modification Algorithm. *IEEE Transactions*, 34(3), May 2004.
9. Park, W., andFaraway, J.J. (2000). Modeling reach motions using functional regression analysis. Digital Human Modeling for Design and Engineering Conference and Exposition, Dearborn, Michigan, June 6-8, 2000.
10. Chaffin, D.B., Faraway, J.J., Zhang, X., and Woolley, C. (2000). Stature, age and gender effects on reach motions postures. *Human Factors, 42*, 408-420.
11. Zhang, X. (1997). Task effects on three-dimensional dynamic postures during seated reaching movements: an investigative scheme and illustration. *Human Factors, 39*(4), 659-671.
12. Hagio, K., Sugano, N., Nishii, T., Miki, H., Otake, Y., Hattori, A., Suzuki, N., Yonenobu, K., Yoshikawa, H., and Ochi, T. (2004). A novel system of four-dimensional motion analysis after total hip athroplasty, *Journal of Orthopaedic Research* 22(3): 665-70.
13. Rahmatalla, S., Kim, H.J., Shanahan, M., and Swan, C.C. (2006). Effect of Restrictive Clothing on Balance and Gait using Motion Capture and Dynamic Analysis, Paper #2005-01-2688, *SAE 2005 Transactions Journal of Passenger Cars-Electronic and Electrical Systems*, March 2006.
14. Miller, C., Mulavara, A., and Bloomberg, J. (2002). A quasi-static method for determining the characteristic of motion capture camera system in a "split-volume" configuration, *Gait & Posture* 16(3): 283-87.
15. Rahmatalla, S, Xia, T., Contratto, M., Kopp, G., Wilder, D., Frey-Law, L., and Ankrum, J. (2008). 3D motion capture protocol for seated operators in whole body vibration", *International Journal of Industrial Ergonomics* 38, 425-433.
16. Della Croce, U., Cappozzo, A., and Kerrigan, D.C. (1999). Pelvis and lower limb anatomical landmark calibration precision and its propagation to bone

geometry and joint angles. *Medical and Biological Engineering and Computing* 37, 155-161.
17. Cappozzo, A., Catani, F., Della Croce, U., and Leardini, A. (1995). Position and orientation in space of bones during movement: Anatomical frame definition and determination. *Clinical Biomechanics* 10(4), 171-178.
18. Gray, H. and Lewis, W.H. (1918). *Anatomy of the Human Body*. Philadelphia, Lea & Febiger.
19. Dempster, W.T. and Gaughran, G.R.L. (1967). Properties of body segments based on size and weight. *American Journal of Anatomy* 120, 33-54.
20. Denavit, J. and Hartenberg, R.S. (1955). A kinematic notation for lower-pair mechanisms based on matrices. *Journal of Applied Mechanics*, 77, 215-221.
21. Gill, P.E., Murray, W., and Saunders, M.A. (2002). SNOPT: An SQP algorithm for large-scale constrained optimization. *SIAM J. OPTIM*.12, 979-1006, 2002.
22. Clopton, N., Schultz, D., Boren, C., Porter, J., and Brillhart, T. (2003). Effects of axial weight loading on gait for subjects with cerebellar ataxia: Preliminary findings. *Neurology Report* 27(1), 15-21.
23. Fulk, G.D. (2004). Locomotor training with body weight support after stroke: The effect of different training parameters. *Journal of Neurologic Physical Therapy.* (28), 20-28.
24. Rahmatalla. S, Xiang, Y., Smith R., Li, J. , Muesch, J. Bhatt, R., Swan, C.C, Arora, J.S., and Abdel-Malek,K. (2008). A validation protocol for predictive human locomotion. SAE Digital Human Modeling Conference, Philadelphia, paper no. 08DHM-0024.2008.
25. Yang, J., Marler, T., and Rahmatalla, S. (2007) Validation methodology development for predicted posture. Paper no. 2007-01-2467, *SAE 2007 Transactions Journal of Passenger Cars - Electronic and Electrical Systems*, 2007.

CONTACT

Corresponding author: Salam Rahmatalla, Ph.D., Assistant Professor, Civil and Environmental Engineering, Center for Computer-Aided Design (CCAD), The University of Iowa, Iowa City, IA 52242, USA. Tel: 319-335-5614, Fax: 319-384-0542.

E-Mail: salam-rahmatalla@uiowa.edu